

Hardware-Based ADMM-LP Decoding

Mitchell Wasson Mario Milicevic Stark C. Draper Glenn Gulak
University of Toronto

Email: m.wasson@mail.utoronto.ca mario.milicevic@utoronto.ca stark.draper@utoronto.ca gulak@eecg.toronto.edu

Abstract—In this paper we present an FPGA-based implementation of linear programming (LP) decoding. LP decoding frames error correction as an optimization problem. This is in contrast to variants of belief propagation (BP) decoding that view error correction as a problem of graphical inference. There are many advantages to taking the optimization perspective: convergence guarantees, improved performance in certain regimes, and a methodology for incorporating the latest developments in optimization techniques. However, LP decoding, when implemented with standard LP solvers, does not easily scale to the blocklengths of modern error-correction codes. In earlier work, we showed that by drawing on decomposition methods from optimization theory, specifically the alternating direction method of multipliers (ADMM), we could build an LP decoding solver that was competitive with BP, both in terms of performance and speed. We also observed empirically that LP decoders have much better high-SNR performance in the “error floor” regime, a trait of particular relevance to optical transport and storage applications. While our previous implementation was in floating point, in this paper we report initial results of a fixed-point, hardware-based realization of our ADMM-LP decoder.

I. INTRODUCTION

The field of error-correction coding was revolutionized in the mid-1990s by the widespread adoption (and academic study) of graph-based codes and associated message-passing decoding algorithms. A key aspect of the success of these codes was their compatibility with hardware. BP-based decoders are naturally distributed algorithms and variants such as Min-Sum are (relatively) easily mapped to hardware. Graph-based codes, particularly turbo codes and low-density parity-check (LDPC) codes, have been adopted in many real world systems.

In the early 2000s, Feldman and his collaborators realized that the maximum likelihood (ML) decoding problem for binary linear codes can be rephrased as an integer program [1]. One obtains an LP by relaxing the integer constraints. Feldman’s results generated much interest among coding theorists. LPs are an extremely well-studied and understood class of optimization problems, especially when contrasted with BP. For instance, LP decoding has an ML certificate property [1]. If LP decoding fails, it fails in a detectable way (to a non-integer vertex) and the relaxation can be tightened and the LP re-run [2]. If a high-quality expander or high-girth code is used, LP decoding is guaranteed to correct a constant number of bit flips [3], [4]. Broadly, it was hoped that by studying LP decoding, more would be understood about BP decoding.

On the practical side, there was less excitement. There initially seemed to be no real-world need for such a decoder, and further, traditional LP solvers did not scale easily to the

blocklengths of modern error-correcting codes. Nevertheless, a number of groups did study how to build an application-specific low-complexity LP decoder [2], [5]–[7]. In particular, Barman et al. built an application-specific LP decoder that was computationally competitive with BP and that had a message-passing structure with a standard message schedule [7]. They solved the LP decoding problem using ADMM, a decomposition technique used in large-scale optimization. Able to study LP decoding performance at long blocklengths, it was observed empirically, and later confirmed theoretically that in the high-SNR regime LP decoders far outperform BP [7]–[9]. In this regime, BP decoders often experience an “error floor” while LP decoders do not. Further, LP decoding can be used as a subroutine in a multi-stage decoder that quickly approaches ML performance [10]. Thus, for application areas in which reliability demands are extreme, LP decoding is an attractive alternative or complement to BP.

However, one major hurdle remains that will determine whether or not ADMM is truly a viable competitor to BP in high-reliability applications. That hurdle is to show that ADMM-LP decoding algorithms can be mapped to hardware without unacceptable performance loss.

In this paper, we present an FPGA-based implementation of an ADMM-LP decoder. First, we review recent developments made to implement the key computational primitive that underlies ADMM in hardware [11]. This primitive is a Euclidean projection onto a particular convex object termed the “parity polytope.” Then we describe how to assemble the pieces to form a complete LP decoder. We present results for a [155, 64, 20] quasi-cyclic (QC) LDPC code introduced by Tanner et al. [12], as well as the [672, 546] QC-LDPC code in the IEEE 802.11ad (WiGig) standard [13]. We test code performance using a full FPGA-based simulation environment. Our initial investigation reveals ADMM-LP decoding in hardware requires more resources than BP-based decoders. However, we also find that it is possible to achieve competitive error rate results with such a fixed-point implementation.

II. BACKGROUND

A. LP Decoding

In this paper, we consider the decoding of binary linear codes. A binary linear code \mathcal{C} can be defined by an $m \times n$ parity-check matrix H as $\mathcal{C} = \{x \in \{0, 1\}^n : Hx = 0 \pmod{2}\}$. Each parity-check matrix row corresponds to a check, which specifies a subset of bits that must add to 0 modulo 2. These checks are indexed by the set $\mathcal{J} = \{1, \dots, m\}$. Each column of the parity-check

matrix corresponds to a codeword symbol or variable indexed by $\mathcal{I} = \{1, \dots, n\}$. The neighborhood of check j , denoted $\mathcal{N}_c(j)$, is the set of variables that check j says must add to 0. That is, $\mathcal{N}_c(j) = \{i : H_{j,i} = 1\}$. Similarly, the neighborhood of variable i , denoted $\mathcal{N}_v(i)$, is the set of checks that variable i participates in.

It was shown that maximum likelihood (ML) decoding of binary linear codes over symmetric memoryless channels is equivalent to the minimization of a linear objective function [1], [14]. The linear objective is formed by creating the vector of log-likelihood ratios γ , where $\gamma_i = \log \left(\frac{p(y_i | x_i=0)}{p(y_i | x_i=1)} \right)$. Here y_i denotes the i^{th} received channel output symbol, and x_i is i^{th} transmitted codeword symbol. The resulting ML decoding problem is $\arg \min_{x \in \mathcal{C}} \gamma^\top x$. Note that γ can be multiplied by any positive scalar without changing the decoding problem.

Let x_S , $S \subseteq \mathcal{I}$ be the length $|S|$ vector formed with the components of x indexed by S . With this notation, we can restate the parity-check condition for a valid codeword as $\mathcal{C} = \{x \in \{0, 1\}^n : 1^\top x_{\mathcal{N}_c(j)} = 0 \pmod{2} \text{ for all } j \in \mathcal{J}\}$. This states that codeword variables connected to a check must be an even-weight vertex of the unit hyper-cube. Linear program (LP) decoding results from relaxing such constraints [1], [14]. LP decoding requires codeword variables connected to a check be in the convex hull of the even-weight vertices of the unit hyper-cube. Visualized in Fig. 1a, the convex hull of the even-weight vertices of the unit hyper-cube is referred to as the parity polytope. The formal definition of the d -dimensional parity polytope, denoted \mathbb{PP}_d , is

$$\mathbb{PP}_d := \text{conv} \left(\left\{ e \in \{0, 1\}^d : 1^\top e = 0 \pmod{2} \right\} \right).$$

With the parity polytope relaxation, LP decoding is the following optimization problem:

$$\begin{aligned} \min_x \quad & \gamma^\top x \\ \text{subject to} \quad & x_{\mathcal{N}_c(j)} \in \mathbb{PP}_{|\mathcal{N}_c(j)|} \quad j \in \mathcal{J} \end{aligned} \quad (1)$$

B. ADMM Decomposition

More recently, a distributed message-passing algorithm to accomplish LP decoding was developed [7]. This algorithm was created by applying the ADMM decomposition technique to LP decoding [15]. The decomposition starts by adding $|\mathcal{J}|$, auxiliary “replica” variable vectors, z_j , for all $j \in \mathcal{J}$. These z_j ’s are length $|\mathcal{N}_c(j)|$ vectors that correspond to the codeword variables participating in check j . Additionally, the constraint that x must be in the unit hyper-cube is added. The result is the equivalent LP:

$$\begin{aligned} \min_{x, z} \quad & \gamma^\top x \\ \text{subject to} \quad & z_j = x_{\mathcal{N}_c(j)} \quad j \in \mathcal{J} \\ & z_j \in \mathbb{PP}_{|\mathcal{N}_c(j)|} \quad j \in \mathcal{J} \\ & x \in [0, 1]^n \end{aligned} \quad (2)$$

where z aggregately refers to the z_j ’s. The decoding algorithm that results from the application of ADMM to (2) is an iterative updating of x and the z_j ’s. After each iteration, an update of the dual variable vectors, λ_j , also occurs. The

development of this algorithm is presented in [7]. We present a slightly modified version of the original algorithm to make the message-passing structure more explicit.

Algorithm 1 ADMM-LP Decoding Algorithm

Input: LLR vector $\gamma \in \mathbb{R}^n$ and iteration cap B

Output: Decoding $x \in [0, 1]^n$

```

1:  $b = 0$ 
2: for all  $j \in \mathcal{J}$  do
3:    $\lambda_j = 0$ 
4:   for all  $i \in \mathcal{I}$  do
5:      $m_{j \rightarrow i} = \frac{1}{2}$ 
6:   end for
7: end for
8: while  $b < B$  do
9:   for all  $i \in \mathcal{I}$  do
10:     $x_i = \prod_{[0,1]} \left( \frac{1}{|\mathcal{N}_v(i)|} (1^\top m_{\mathcal{N}_v(i) \rightarrow i} - \gamma_i) \right)$ 
11:   end for
12:   for all  $j \in \mathcal{J}$  do
13:     $v = x_{\mathcal{N}_c(j)} + \lambda_j$ 
14:     $z = \prod_{\mathbb{PP}_{|\mathcal{N}_c(j)|}} (v)$ 
15:     $\lambda_j = v - z$ 
16:     $m_{j \rightarrow \mathcal{N}_c(j)} = 2z - v$ 
17:   end for
18:    $b = b + 1$ 
19: end while
20: return  $x$ 

```

In Algorithm 1, we use the notation $m_{\mathcal{N}_v(i) \rightarrow i}$ to refer to the length $|\mathcal{N}_v(i)|$ vector whose components are the messages sent to variable i from its neighbors. Similarly, $m_{j \rightarrow \mathcal{N}_c(j)}$ refers to the length $|\mathcal{N}_c(j)|$ vector whose components are the messages from check j to its neighbors.

This presentation of the decoding algorithm shows that messages are passed between variable and check computations in a manner similar to BP-based decoding. There are two differences in the message-passing structure though. The first is that variable i sends the same message x_i to all its neighbors. The second is the addition of the dual variable vectors λ_j . These vectors serve as an internal state for checks.

We also have an intuition for the operations performed in the variable and check updates. The variable update (step 10) is an averaging operation of all incoming messages along with the channel information. The average is then projected onto the feasible set for x . Check computations correspond mainly to a projection onto the parity polytope to enforce code constraints (step 14). The λ_j ’s are incorporated into these projections to achieve faster convergence by indicating how the check has been violated in the past.

Projecting onto the parity polytope is the essential nontrivial primitive in ADMM-LP decoding. We review this projection and overview an algorithm that accomplishes it.

The parity polytope is a polyhedron. Therefore, projecting a point $v \in \mathbb{R}^d$ onto \mathbb{PP}_d is given by a quadratic program,

$$\prod_{\mathbb{PP}_d} (v) := \arg \min_{z \in \mathbb{PP}_d} \|v - z\|_2^2.$$

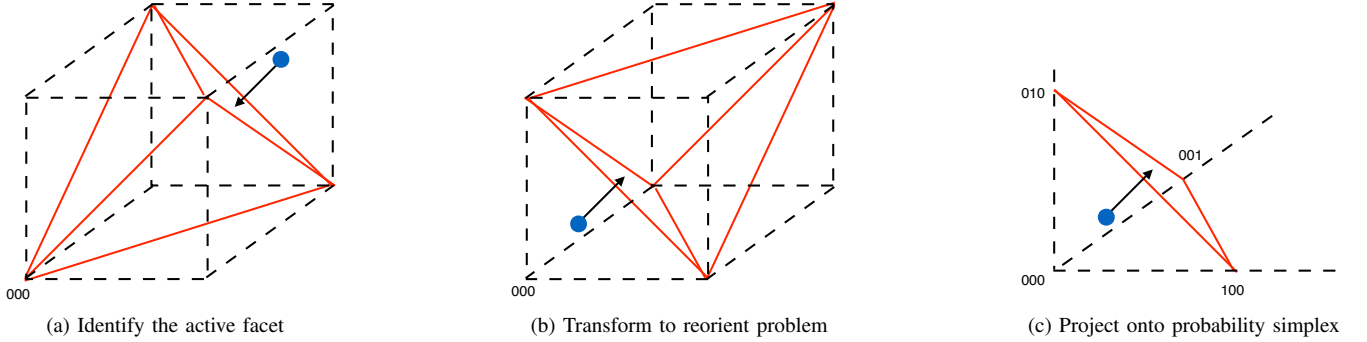


Fig. 1: Projection onto the parity polytope \mathbb{PP}_3 : Identify the active facet, similarity transformation, simplex projection.

Barman et al. developed a routine for projection onto \mathbb{PP}_d [7]. Follow-up work by X. Zhang and Siegel provided a new approach based on identifying the facet of the polytope to be projected onto [16]. Additionally, G. Zhang et al. made improvements by reducing the parity polytope projection to a projection onto the probability simplex [17]. In a previous work, we extracted the best features of these new algorithms and proved their compatibility [11]. This results in a new projection method appropriate for hardware. Our approach uses a parallizable method for efficient projection onto the d -dimensional probability simplex [18].

Fig. 1 displays the geometric interpretation of the parity polytope projection algorithm developed in [11]. First, the facet of the polytope on which the projection lies is identified with the cut-search algorithm of [19]. Then, a similarity transform, derived from that developed in [17], is performed using this information. This reduces the parity polytope projection to a projection onto the probability simplex. After the simplex projection, the transform is inverted to obtain the final projection onto the parity polytope.

Our previous study revealed how to achieve a fully parallel hardware implementation of the projection algorithm using primitives like sorting networks and prefix sum operations [11]. The hardware implementation achieves an area scaling on the order of $\mathcal{O}(d(\log d)^2)$ with a delay scaling of $\mathcal{O}((\log d)^2)$, where d is the projection dimension.

III. HARDWARE ARCHITECTURE

In the previous section, we showed that ADMM-LP decoders implement a message-passing schedule similar to BP decoders, one that is based on the implied check and variable node connectivity structure defined by the binary parity-check matrix. This similarity allows us to build upon well-known hardware architectures used for BP decoders in the design of a hardware-based ADMM-LP decoder implementation. We modify the arithmetic kernels in the check and variable processing nodes as per the operations outlined in Algorithm 1.

A. Architecture Selection for FPGA Platform

Hardware architectures for BP decoders have been studied extensively over the past 15 years, and can be classified

into one of the following three architectures: fully-parallel, partially-parallel, and serial. Fully-parallel decoders achieve high data throughput at the expense of high area/computational resource utilization, while serial decoders require minimal area but suffer from high latency [20], [21]. Partially-parallel decoders provide the most optimal trade-off between area resource utilization and data throughput [22], and are generally well-suited for FPGA implementation since power consumption is not a crucial metric for this work.

The goal of this work is to develop a platform enabling accelerated ADMM-LP decoding in order to study the error correction performance of a wide variety of linear binary codes. An FPGA-based platform provides a re-programmable and cost-effective solution. Once a code's performance is well-understood, a custom, energy-efficient architecture can later be explored for silicon-based integrated circuit implementation. In this work, however, we sacrifice the power, area, and throughput design objectives to create a more general implementation that can rapidly be applied to study new codes. This work therefore implements a partially-parallel decoder architecture, which allows us to take advantage of the high availability of FPGA slice registers for deep pipelining to minimize decoding latency, while operating within the fixed logic and routing resource limitations of the target FPGA.

B. Partially-Parallel Decoder Implementation

A central challenge in implementing hardware-based decoders is the scalability of the message-passing network, which often requires resource-intensive wiring and memory interconnect resources to pass messages between check node (CN) and variable node (VN) processing units. The partially-parallel architecture allows us to minimize FPGA routing complexity by implementing the message-passing network with regularly-distributed, on-chip FPGA block RAMs. Fig. 2 presents an overview of our partially-parallel QC-LDPC decoder architecture. The architecture is comprised of multiple memory types to store input LLRs, intermediate messages, and output codewords, as well as pipelined CN and VN processing units that perform the arithmetic operations used in Algorithm 1.

We restrict ourselves to quasi-cyclic (QC) codes [23], [24] in order to simplify message routing and memory interfacing.

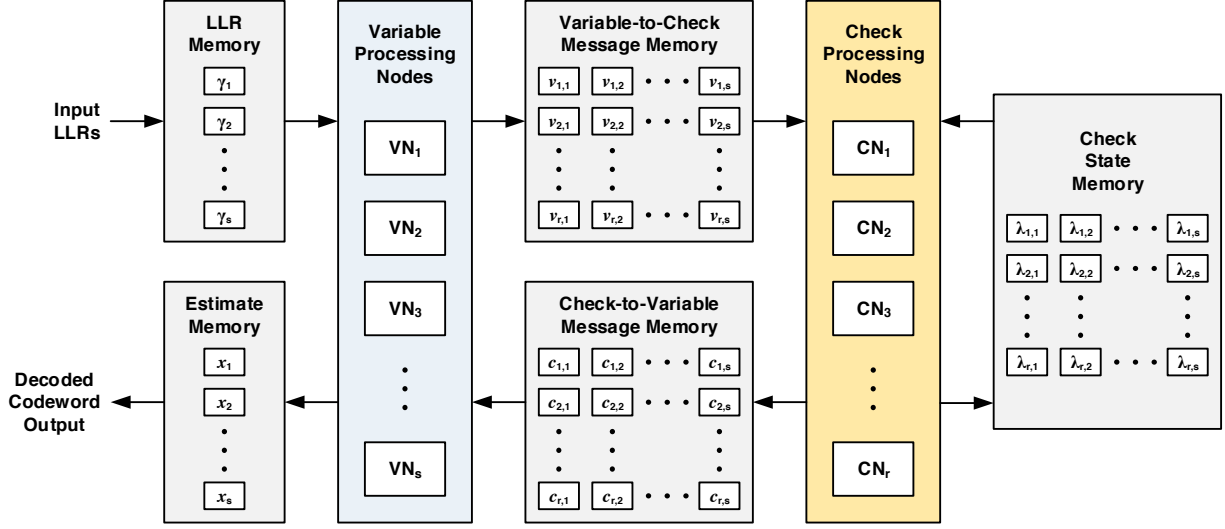


Fig. 2: Partially-parallel decoder architecture.

QC codes are defined by a parity-check matrix formed by tilings of $p \times p$ circulant matrices. Therefore, each tile of a QC parity-check matrix can either be the all-zeros matrix or some addition of shifted-identity matrices. The tilings naturally divide the parity-check matrix into $s := \frac{n}{p}$ “proto”-columns and $r := \frac{m}{p}$ proto-rows. Inside a given proto-row (column), the required message locations for a check (variable) computation are the locations for the previous check (variable) plus 1 modulo p . This rich class of codes is popular in hardware implementations, appearing in standards such as IEEE 802.11ad (WiGig) [13].

The first execution step our decoder performs is to load channel LLRs into memory. We instantiate s memories, each of depth p to store the LLRs. Each of these memories is then read in parallel to feed LLRs into s pipelined VNs. The VNs also receive messages from a check-to-variable (CN-to-VN) message memory, to be discussed later. At the output of the VNs, the current variable estimates (the x_i ’s) are written into s estimate memories in parallel, to be read from upon decoding termination. Additionally, variable estimates are written into variable-to-check (VN-to-CN) message memories. There is a VN-to-CN message memory for each shifted-identity matrix used to construct the parity-check matrix. These memories are addressed using their corresponding shift number to ensure the messages are passed to the proper CN.

Next, r pipelined CNs read their required messages in parallel from the VN-to-CN message memory. Additionally, the check states are read from check state memories, which are instantiated in the same manner as the VN-to-CN message memories. However, address shifting is not required since these memories are only written to, and read by, CNs. When a CN computation completes, the new check states are written back into the check state memory and the messages are written into CN-to-VN message memories. These message memories are again structured in the same manner with write operations using cyclic shift information. The process repeats until the

maximum number of iterations is exceeded, or some early termination condition is satisfied.

C. Fixed-Point Message Quantization

In our current implementation, we have found the ADMM-LP decoder to be sensitive to fixed-point quantization. In contrast to BP decoders, which can be implemented with 5 or 6-bit variable widths with minimal degradation in bit-error-rate performance compared to floating point [25], ADMM requires larger bit-widths. We believe that the ADMM-LP decoder requires higher precision because the result of the projection operation that check nodes perform must be quantized. This results in a loss of precision and a corresponding deterioration of message resolution.

We now discuss some intuition behind the choices we made in picking fixed-point representations. We first note that a change in the assignment of bits between integer and fraction parts of fixed-point LLRs amounts to a linear scaling of the objective. However, any scaling of the objective in an LP (i.e., of γ in (1)) does not change the solution of the LP. This provides some flexibility in choosing the fixed-point representation of the LLRs. Next we note that each message passed to a variable node can be thought of as either trying to overcome the channel information or as trying to reinforce it. Thus, any extra bit-width should be allocated to the integer part of a CN-to-VN message. This provides dynamic range to override channel LLRs. In contrast, any extra bit-width allocated to VN-to-CN messages should be fraction bits. An increase in the number of fraction bits mitigates the effect of the inexact (due to finite precision) normalization by $|\mathcal{N}_{v(i)}|$ in the variable nodes (cf. step 10 of the Algorithm).

Based on the above design intuition, we select fixed-point message representations based on the premise of retaining as much channel information as possible. First, we consider the bit-width for both the LLRs and the estimate outputs. These, respectively, correspond to the decoder’s input and output

message widths. Next, we consider how many additional bits VN-to-CN and CN-to-VN messages will receive. VN-to-CN messages, as well as the estimates, lie in the unit hyper-cube. Therefore, these messages receive one sign bit, one integer bit, and allocate the remainder to fraction bits. Next, we give LLRs one sign bit, zero integer bits, and allocate the remainder to fraction bits. This ensures that all channel information is visible in the estimates and the VN-to-CN messages. The CN-to-VN messages are given one sign bit and the same number of fraction bits as the LLRs. This is done so that the summation in the VN computation produces an output that does not have any constant bits for some given LLR. Finally, the check states are given the same representation as the CN-to-VN messages because they are computed in a similar manner.

The next section presents the error-correction performance results for our FPGA-based ADMM-LP decoder for two different linear block codes. We also explore the resources required by this architecture on a state-of-the-art FPGA.

IV. RESULTS

A. Performance

In order to test the hardware viability of ADMM-LP decoding, we developed an FPGA-in-the-loop simulation environment using an Xilinx Virtex 5 FPGA. The proposed architecture was synthesized for the FPGA along with logic for random number generation and data transfer.

The binary-input AWGN channel was simulated using a synthesized Gaussian random number generator [26]. The core is a linear feedback shift register with period 2^{176} fed into an inverse cumulative distribution function approximation. The output of the simulated channel was saturated at one standard deviation of channel noise to create LLRs within the decoder's input range. This on-FPGA method of channel simulation was necessary since generating channel outputs on a PC and transferring them to the FPGA became a simulation bottleneck. We verified that the on-FPGA method produced equivalent channel simulations for the decoder configuration we present.

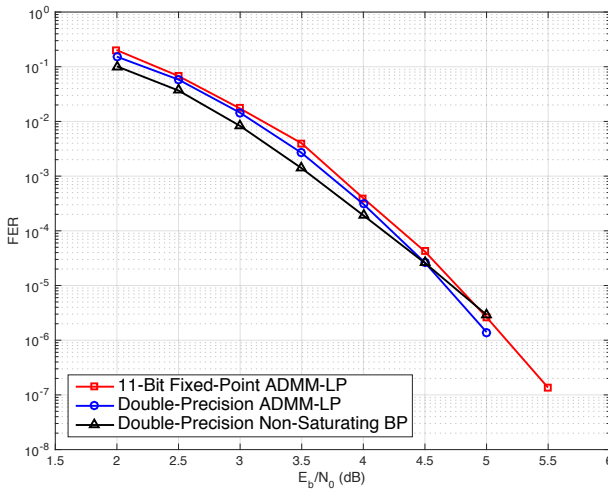


Fig. 3: FER performance of the $[155, 64]$ ‘‘Tanner’’ code.

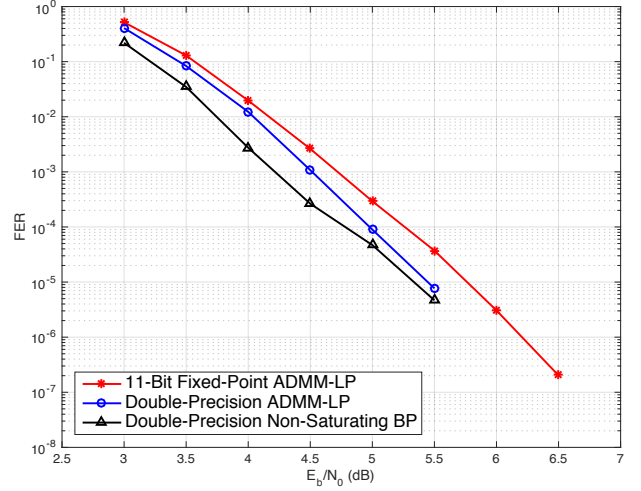


Fig. 4: FER performance of the WiGig code.

Both the aforementioned $n = 155$, rate $64/155$ code given by Tanner and the $n = 672$, rate $13/16$ WiGig code were used to test the fixed-point ADMM-LP hardware implementation. We configured our implementation to receive 8-bit LLRs and pass 11-bit messages internally. Both codes were also simulated using double-precision ADMM-LP and non-saturating sum-product BP decoding [27]. All implementations were run for a maximum of 500 iterations and each point shown on the plots is an accumulation of at least 100 frame errors.

Fig. 3 shows that the fixed-point implementation of ADMM-LP decoding produces error rates extremely close to double-precision implementations, even surpassing double-precision BP at a high SNR. Fig. 4 displays similar competitive error rates for the WiGig code.

One observed effect of the fixed-point implementation we noted is a slight codeword asymmetry. Specifically, for small bit-widths, the all-zeros codeword achieved a lower FER than higher-weight codewords. The effect is due to numerical truncation rounding toward negative infinity. Further investigation, not shown in this paper, suggests that including rounding operations as well as centering estimates about zero resolves the codeword asymmetry problem. However, due to this effect, we use high-weight codewords in the displayed simulations.

B. Resource Utilization

We now detail the resources required to synthesize the decoder on a state-of-the-art FPGA. The FPGA used in the following resource estimates is an Altera Stratix V FPGA (model 5SGXEA7N2F45C2). This FPGA has 234,720 adaptive logic modules (ALMs), 256 dedicated DSP blocks, and 2,560 M20K RAM blocks.

First we consider synthesizing the decoder architecture for the Tanner code. This is a regular QC-LDPC code with degree-5 check and degree-3 variable nodes. The parity-check matrix is composed of three proto-rows and five proto-columns. Therefore the decoder is composed of five degree-3 variable nodes and three degree-5 check nodes.

The WiGig code is also quasi-cyclic. However, some tiles of the parity-check matrix are all-zeros. Therefore this code is irregular. This results in an implementation with fourteen degree-3 variable nodes, one degree-2 variable node, and one degree-1 variable node. Additionally, there is one degree-16 check node, one degree-15 check node, and one degree-14 check node.

Module	ALM (%)	DSP (%)	RAM (%)	Period (ns)	Pipeline Stages
Tanner Dec.	5.28	4.30	1.64	4.72	-
Deg. 3 VN	0.06	0.39	0	4.72	10
Deg. 5 CN	1.48	0.78	0	4.72	46
WiGig Dec.	15.06	17.97	3.59	4.58	-
Deg. 1 VN	0.02	0	0	4.58	9
Deg. 2 VN	0.03	0	0	4.58	10
Deg. 3 VN	0.03	0.39	0	4.58	10
Deg. 14 CN	4.37	3.91	0	4.58	53
Deg. 15 CN	4.67	4.30	0	4.58	53
Deg. 16 CN	5.11	4.30	0	4.58	54

TABLE I: Resource utilization table for Altera Stratix V.

Table I displays the percentage of on-FPGA resources required to synthesize the decoders for each of the two codes (cf. the bolded rows labeled “Tanner Dec.” and “WiGig Dec.”). We also give numbers for each of the important sub-modules. The clock period of the synthesized circuit (which is constant for all modules in a given decoder), and the number of pipeline stages for sub-modules, are also provided.

V. CONCLUSION

This work presented an early investigation into the feasibility of a hardware-based ADMM-LP decoder. We target an FPGA platform with fixed logic, memory, and routing resources. We showed that an FPGA-based, partially-parallel, decoder architecture can be used to study ADMM-LP decoding performance of linear block codes shorter than 1000 bits. We now mention some future work. The first is the full understanding (and elimination) of the codeword asymmetry mentioned. The second is further investigation of error-floor regime performance for LP (and penalized-LP [28]) decoding. A third is the development of simplified decoding algorithms that maintain error-floor performance while reducing the required bit-width. Our ultimate objective is a fully-custom silicon integrated circuit implementation, which would be required to achieve decoding speedup for longer codes. In such an implementation, it would be beneficial to explore new hardware architectures that would provide greater information throughput, and parity-check matrix reconfigurability.

REFERENCES

- [1] J. Feldman, M. J. Wainwright, and D. R. Karger, “Using linear programming to decode binary linear codes,” *IEEE Trans. Inf. Theory*, vol. 51, no. 3, pp. 954–972, Mar. 2005.
- [2] M. H. Taghavi and P. H. Siegel, “Adaptive methods for linear programming decoding,” *IEEE Trans. Inf. Theory*, vol. 54, no. 12, pp. 5396–5410, Nov. 2008.
- [3] J. Feldman, T. Malkin, R. A. Servedio, C. Stein, and M. J. Wainwright, “Message-passing algorithms and improved LP decoding,” in *Proc. Int. Symp. Inf. Theory*, Chicago, IL, Jun. 2005.

- [4] A. Arora, D. Steuer, and C. Daskalakis, “Message-passing algorithms and improved LP decoding,” in *ACM Symposium on Theory of Computing (STOC)*, May 2009.
- [5] P. O. Vontobel and R. Koetter, “Towards low-complexity linear-programming decoding,” in *Proc. 4th Int. Symp. Turbo Codes and Related Topics*, Munich, Germany, Apr. 2006, pp. 1–9.
- [6] D. Burshtein, “Iterative approximate linear programming decoding of LDPC codes with linear complexity,” *IEEE Trans. Inf. Theory*, vol. 55, no. 11, pp. 4835–4859, Nov. 2009.
- [7] S. Barman, X. Liu, S. C. Draper, and B. Recht, “Decomposition methods for large scale LP decoding,” *IEEE Trans. Inf. Theory*, vol. 59, no. 12, pp. 7870–7886, Dec. 2013.
- [8] X. Liu and S. C. Draper, “Instanton search algorithm for the ADMM penalized decoder,” in *Proc. Int. Symp. Inf. Theory*, Honolulu, Jun. 2014.
- [9] —, “ADMM decoding on trapping sets,” in *Proc. Int. Symp. Inform. Theory*, Hong Kong, Jun. 2015.
- [10] Y. Wang, J. S. Yedidia, and S. C. Draper, “Multi-stage decoding of LDPC codes,” in *Proc. Int. Symp. Inf. Theory*, South Korea, Jul. 2009.
- [11] M. Wason and S. C. Draper, “Hardware based projection onto the parity polytope and probability simplex,” in *Proc. 49th Asilomar Conf. Signals, Systems, Computers*, Pacific Grove, CA, Nov. 2015, pp. 1015–1020.
- [12] R. M. Tanner, D. Sridhara, and T. Fuja, “A class of group-structured LDPC codes,” in *Proc. ICSTA*, Ambleside, U.K., Jul. 2001.
- [13] “IEEE Standard for Information technology—Telecommunications and information exchange between systems—Local and metropolitan area networks—Specific requirements—Part 11: Wireless LAN Medium Access Control and Physical Layer Specifications Amendment 3: Enhancements for Very High Throughput in the 60 GHz Band,” *IEEE Std 802.11ad-2012 (Amendment to IEEE Std 802.11-2012, as amended by IEEE Std 802.11ae-2012 and IEEE Std 802.11aa-2012)*, pp. 1–628, Dec 2012.
- [14] J. Feldman, “Decoding error-correcting codes via linear programming,” Ph.D. dissertation, MIT, MA, USA, 2003.
- [15] S. Boyd, N. Parikh, E. Chu, B. Peleato, and J. Eckstein, “Distributed optimization and statistical learning via the alternating direction method of multipliers,” *Machine Learning*, vol. 3, no. 1, pp. 1–122, 2011.
- [16] X. Zhang and P. H. Siegel, “Efficient iterative LP decoding of LDPC codes with alternating direction method of multipliers,” in *Proc. IEEE Int. Symp. Inf. Theory*, Istanbul, Turkey, Jul. 2013, pp. 1501–1505.
- [17] G. Zhang, R. Heusdens, and W. B. Kleijn, “Large scale LP decoding with low complexity,” *IEEE Commun. Lett.*, vol. 17, no. 11, pp. 2152–2155, Nov. 2013.
- [18] J. Duchi, S. Shalev-Shwartz, Y. Singer, and T. Chandra, “Efficient projections onto the ℓ_1 -ball for learning in high dimensions,” in *Proc. Int. Conf. Machine Learning*, San Diego, CA, USA, Dec. 2008.
- [19] X. Zhang and P. H. Siegel, “Adaptive cut generation algorithm for improved linear programming decoding of binary linear codes,” *IEEE Trans. Inf. Theory*, vol. 58, no. 10, pp. 6581–6594, Oct. 2012.
- [20] A. Blanksby and C. Howland, “A 690-mW 1-Gb/s 1024-b, rate-1/2 low-density parity-check code decoder,” *IEEE J. Solid-State Circuits*, vol. 37, no. 3, pp. 404–412, Mar. 2002.
- [21] T. Bhatt, V. Sundaramurthy, V. Stolzman, and D. McCain, “Pipelined block-serial decoder architecture for structured LDPC codes,” in *Proc. Int. Conf. Acoustics, Speech Signal Proc.*, May 2006.
- [22] D. E. Hocevar, “A reduced complexity decoder architecture via layered decoding of LDPC codes,” in *Proc. Work. Signal Proc. Systems*, Oct. 2004.
- [23] Y. Kou, S. Lin, and M. P. C. Fossorier, “Low-density parity-check codes based on finite geometries: a rediscovery and new results,” *IEEE Trans. Inf. Theory*, vol. 47, no. 7, pp. 2711–2736, 2001.
- [24] M. P. C. Fossorier, “Quasicyclic low-density parity-check codes from circulant permutation matrices,” *IEEE Trans. Inf. Theory*, vol. 50, no. 8, pp. 1788–1793, 2004.
- [25] Y. S. Park, D. Blaauw, D. Sylvester, and Z. Zhang, “Low-power high-throughput LDPC decoder using non-refresh embedded DRAM,” *IEEE J. Solid-State Circuits*, vol. 49, no. 3, pp. 783–794, Mar. 2014.
- [26] G. Liu, Gaussian noise generator. OpenCores. [Online]. Available: http://opencores.org/project_gng
- [27] B. K. Butler and P. H. Siegel, “Error floor approximation for LDPC codes in the AWGN channel,” *IEEE Trans. Inf. Theory*, vol. 60, no. 12, pp. 7416–7441, Dec. 2014.
- [28] X. Liu and S. C. Draper, “The ADMM penalized decoder for LDPC codes,” *IEEE Trans. Inf. Theory*, 2016.